

RESEARCH ARTICLE

PneuNetV1: A Deep Neural Network for Classification of Pneumothorax Using CXR Images

MAHENDRA KUMAR GOURISARIA¹, (Member, IEEE), VINAYAK SINGH¹,
RAJDEEP CHATTERJEE¹, SANJAYA KUMAR PANDA², (Senior Member, IEEE),
MANAS RANJAN PRADHAN³, (Member, IEEE),
AND BISWARANJAN ACHARYA⁴, (Senior Member, IEEE)

¹School of Computer Engineering, KIIT Deemed to be University, Bhubaneswar, Odisha 751024, India

²Department of Computer Science and Engineering, National Institute of Technology at Warangal, Warangal, Telangana 506004, India

³School of Computing, Skyline University College, Sharjah, United Arab Emirates

⁴Department of Computer Engineering–Artificial Intelligence and Big Data Analytics, Marwadi University, Rajkot, Gujarat 36003, India

Corresponding authors: Biswaranjan Acharya (biswaacharya@ieee.org) and Mahendra Kumar Gourisaria (mkgourisaria2010@gmail.com)

ABSTRACT Pneumothorax is a critical medical condition among human-beings. A severe pneumothorax causes collapsed lungs. It is a life-threatening disease. Therefore, pneumothorax detection is an important step for the prevention and curing of a patient. Pneumothorax can be classified into three major categories: primary, secondary, and injury. Magnetic resonance imaging (MRI)-based digital imaging and communications in medicine (DICOM) files of Chest X-ray (CXR) images provide insight and help the doctor to make an appropriate decision. An early decision can prevent the mortality rate among patients. Since the outbreak of the COVID-19 pandemic, the medical systems and staff have gone under massive pressure. Classification from a CXR image by an expert requires huge manpower and a longer time to determine. Deep learning-based automatic classification of Pneumothorax (CXR) images can assist the medical community in a fast diagnosis and reduce the burden of work overload. Doctors can focus on better treatment and cure of Pneumothorax. In this paper, we have proposed seven scratch Convolutional Neural Networks (CNN) architectures and compared them with another seven transfer learning models. The best-performing CNN model (PneuNetV1) is determined based on various standard performance metrics. It has gained the highest test accuracy, efficacy ratio, and F1-score of 0.9123, 5.2370, and 0.9220, respectively with a minimum training time. The obtained results are achieved through rigorous experimentation and yet provide satisfactory performance.

INDEX TERMS Convolutional neural network (CNN), CXR images, pneumothorax, transfer learning, VGG-19.

I. INTRODUCTION

Over the past few decennaries, cases of lung diseases have increased rapidly. The presence of air in the pleural space of the lungs is defined as Pneumothorax. Homo sapiens have been facing pneumothorax as a common clinical health problem. Lungs are essential air-filled organs of the human body which is set of spongy, positioned on both sides of

The associate editor coordinating the review of this manuscript and approving it for publication was Yongming Li¹.

the thorax (chest). Lungs consist of Trachea which works as the passage for inhaled air into the lungs through its tubular branches known as bronchi. Bronchi consist of small bronchioles which are microscopic. Similarly, Alveoli are air sacs that consist of clusters of bronchioles [1].

Humans have suffered from various lungs diseases such as chronic obstructive pulmonary disease (COPD), Pneumonia, Asthma, Sarcoidosis, pulmonary fibrosis, lung cancer, tuberculosis, influenza, etc. Pneumothorax occupies the largest proportion of lungs related diseases. This problem occurs

when air enters the area around the lungs abnormally [1]. These situations related to pneumothorax might occur due to ruptured air blisters, lung disease, mechanical ventilation, any accident, or any internal injury which can directly impact on lungs. Pneumothorax is also known as collapsed lung disease. In this severe condition air leaks into the space present between the chest wall and lungs. Pneumothorax consists of two states wherein in one state a lung can completely collapse and in another one, only a portion of the lung gets collapsed. It can be classified into binary categories: Traumatic pneumothorax and Non-traumatic pneumothorax where traumatic appears due to an internal injury while non-traumatic are closely related to peoples who smoke, Marfan syndrome, during pregnancy, lung diseases like COPD, lung cancer, asthma, cystic fibrosis, and other diseases. Smoking, genetics, and previous pneumothorax are various risk factors associated with pneumothorax. A minor error in the proper diagnosis may result in disastrous repercussions. So in terms of treatment for a pneumothorax usually comprises of insertion of a needle or chest tube between the ribs to remove the extra excess air present inside the lungs. In small cases related to pneumothorax, it may heal on its own. After considering a long-term scenario for pneumothorax it can create a huge impact but results may vary.

Pneumothorax is a curable disease but it also depends on various aspects such as the current condition of the disease, whether the cavity is expanding, the cause of pneumothorax, and many other factors that impact the treatment condition related to pneumothorax. Various techniques like draining excess air, surgery via using thoracoscopy, various surgery techniques like sewing blisters closed, closing the air leakage path, and removal of the portion related to collapsed lungs known as lobectomy. For better diagnosis, various medical imaging like CT scan, X-ray, and thoracic ultrasound plays an essential role in the segmentation of pneumothorax. In the current scenario, the modern problem requires modern solutions so various niche areas like machine learning and deep learning play an important role in the diagnosis of various diseases like diabetes by supervised algorithms [2], [3], pneumonia by using multimodal deep learning techniques [4], liver diseases by using various boosting and supervised techniques [5], Alzheimer disease by using convolutional neural networks [6], arrhythmia detection by using deep belief network and supervised methodologies [7], COVID 19 detection by utilizing federated machine learning [8] and chronic kidney by using various standard machine learning algorithms [9].

Most of the researchers have focused on the segmentation and detection of pneumothorax, but they lack in terms of rigorous experiments based on wide range of evaluation metrics. Some proposed architectures are not well analyzed and training has been performed on small datasets. Here, we overcome the problem associated with all other studies in terms of performance evaluation and size of the dataset (more than ten thousands images). Many researchers have

also contributed for the classification of pneumothorax but most of them were concentrated towards the highest classification accuracy but this paper emphasizes on low computational cost deep learning architecture for classification with outstanding results. So, in this research article, we have proposed a Convolutional Neural Network for the classification of pneumothorax. We have designed scratch CNN models to compare with other widely used SOTA CNN models. In classification, our proposed PneuNetV1 performs better on the used pneumothorax dataset. In addition, the PneuNetV1 takes less training time to reach best performances from the CXR images over other CNN architectures.

The paper is divided into five sections. Section II deals with literature review whereas Section III deals with the materials and methods related to this study, Section IV discusses the results and provide an analysis of work done, and Section V provides the discussion section which shows the better aspects related to the proposed work and its comparison with other related work, and finally Section VI deals with a conclusion and future work of pneumothorax. This real-world deployment will lead us to propose a low computational cost framework for better analysis and diagnosis of pneumothorax.

II. LITERATURE REVIEW

Many researchers have contributed to solve the problem. Deep learning can provide an efficient classification and detection pneumonia using a convolutional neural network [10], EEG signal classification [11], [12], and various medical diseases and problems [13]. Similarly, many researchers have also contributed to the domain of pneumothorax such as Kitamura and Deible [14] trained a machine learning model on the CXR image dataset for the classification of pneumothorax from non-pneumothorax CXR images and they achieved an area under the curve of 0.90 and inference on validation set achieved an area under the curve of 0.59. The dataset contained a training set of 41946 images for the non-pneumothorax class and 4696 for the pneumothorax class while the validation set was 11120 for the non-pneumothorax class and 54 for the pneumothorax class. Chan et al. [15] have proposed an automatic method for segmentation of pneumothorax where they used a support vector machine (SVM) for classifying the pneumothorax class. Feature extraction has been carried out by using the local binary pattern technique. The proposed architecture is based on multiscale intensity texture segmentation. They also diagnosed and recognized the boundaries of ribs via Sobel edge detection. They have achieved an accuracy of 0.858, a precision value of 0.836, and a sensitivity of 0.874 via a patch size of 5×5 .

AUC of 0.98 has been achieved by Röhrich et al. [16] by proposing an automatic detection system that can quantify pneumothorax by using CT scans. They proposed a UNet architecture and dataset containing 43 CT scans and for testing 9 CT scans have been considered for

pixel-based annotation while 567 Computed tomography scans are based on volume level. The evaluation is concentrated on automated, volume-level pneumothorax grading and pixel-level classification. In their results, they achieved an average precision value of 0.97 and a dice similarity coefficient of 0.92. Similarly, Li et al. [17] proposed a deep learning-based image classification system for the diagnosis and detection of pneumothorax via computed tomography scans. In their study, they proposed a Convolutional neural network (CNN) of 8 layers which consisted of 2D image patches of size (36 x 36) pixels, and training was performed on 80 CXR CT scans were 62.5% of the data has been consisting pneumothorax class while rest 37.5% is from non-pneumothorax class. Test data contains 200 CT scans where 160 images are with pneumothorax and 40 images are considered as a non-pneumothorax class. In terms of performance, they achieved a sensitivity of 100% and specificity of 82.5%.

Taylor et al. [18] have used 13292 images to propose an automatic detection of pneumothorax by using deep convolutional neural network architecture. Their dataset contains 3107 positive classes. They have compared the deep neural architectures in terms of sensitivity, the area under the curve, and specificity. On analysis, they achieved a sensitivity score of 0.84, 0.94 for AUC, and a specificity of 0.90. In terms of the high specificity model, they had a sensitivity of 0.80, AUC-ROC of 0.96, and specificity of 0.97. They also have performed testing on the NIH dataset but the results are not satisfactory in terms of performance metrics.

Collapsed lungs are diagnosed by Lindsey et al. [19] by using deep transfer learning architectures and they proposed a tChexNet with 122 layers and trained this architecture from scratch. They have used the technique of transferring weights from CheXNet to tChexNet and they have achieved an AUC of 10% better than the CheXNet on the testing set. Dataset is distributed into three categories: a training set with 94,482 images, a validation set of 23,620 images, and a 202 testing set. The receiver operating characteristic – area under the curve (ROC - AUC) achieves the value of 0.708 for the classification and detection of pneumothorax. The results are good but the performance on the test set is poor and comprehensive. Table 1 shows the tabular comparison of related works of pneumothorax concerning their advantages and disadvantages. From the above studies, we can conclude that machine learning and deep learning is playing an essential role in medical fields as they are solving major chunks of problems like sperms classification [20], Parkinson's disease [21], brain tumor [22], skin lesion [23] and predicting depression [24] efficiently.

In recent studies, Hong et al. [25] have proposed a deep learning-based computer-aided detection system in clinical practice improved the diagnostic performance for detecting pneumothorax. It has performed on 1352 chest radiographs from 1319 patients. Lee et al. [26] have introduced a deep learning based pneumothorax detection through an electrocardiogram. It includes 107 ECG signal data from 98 pneumothorax patients.

Feng et al. [27] used CANDID-PTX dataset for the segmentation and classification of pneumothorax where they evaluated model on the basis of AUC-ROC, specificity and sensitivity whereas true positive dice coefficient and mean dice were considered as performance metrics for segmentation. Best model achieved an AUC-ROC of 0.94 with specificity of 0.95 and sensitivity of 0.93. Tian et al. [28] used the power of transfer learning paradigm ResNet for 2 stage strategy for identification of pneumothorax by using dual dataset approach. They achieved an accuracy of 0.94 and F1 score of 0.94 by a state of the art (SOTA) architecture on NIH dataset. Kumar et al. [29] propose PneuNet, an ensemble deep learning model for pneumothorax detection. PneuNet addresses class disparity through data augmentation and utilizes a segmentation system to identify dark areas. The model achieves an accuracy of 98.41% on the pneumothorax dataset, outperforming other deep learning models.

III. MATERIALS AND METHODS

The following section discusses the materials and methodology used for the classification of pneumothorax on CXR images. The section is divided into seven sub-sections where Section III-A deals with the original dataset used for this study, Section III-B deals with the in-depth analysis of the original dataset, Section III-C discusses the data augmentation and preprocessing, Section III-D, III-E, and III-F deal with methodologies used such as Convolutional Neural Network, Artificial Neural Network, and Transfer Learning models, and Section III-G discusses about the software and hardware used for classification of pneumothorax.

A. DATASET USED

The pneumothorax dataset used for this study has been taken from Kaggle which was deployed by Abhishek Thakur [30]. Dataset author has generated all these images from a Kaggle competition and the dataset contained binary categories, Pneumothorax and Non-Pneumothorax class. In terms of ground truth, images are in the form of a DICOM file. For our case, we converted DICOM images into .jpg format for classification. Figure 1 shows the sample of the CXR image from the dataset. The original dataset consisted of 12,089 DICOM images.

B. DATASET VISUALIZATION

In this section, we explored and analyzed the details related to the DICOM images. Various insights were gathered from these graphs. Figure 2 shows the graph where 77.6% of the majority class consists of non-pneumothorax CXR DICOM files and the rest 22.4% are pneumothorax CXR DICOM files. From Figure 2 we can also observe the imbalance nature in the classes as it will lead to developing a model which will be highly inclined towards non-pneumothorax classification. So for further consideration and analysis, we need an image augmentation technique that will help to resolve the issue of the imbalanced nature of class labels. Figure 3

TABLE 1. Tabular representation of literature review.

| Author Name | Advantages | Disadvantages |
|----------------------------|--|---|
| Kitamura et al. (2020) [9] | AUC-ROC was very high. Dataset was very good in terms of size. | No segmentation was performed. No other performance metrics were considered. |
| Chan et al. (2018) [10] | Propose work was good. Extraction and classification were well explained. | Dataset was very small in size. No comparative results were included. The results gained were also not so good. |
| Rohrich et al. (2020) [11] | The results were very good. The proposed work was efficient. | Dataset used was very small. |
| Li et al. (2019) [12] | The results were good. CNN architecture performed well. | Lacked in the comparative study. Dataset was imbalanced. |
| Taylor et al. (2018) [13] | Testing was performed on large scale. Architecture gave good performance metrics. | Dataset was inclined towards non-pneumothorax classes. |
| Lindsey et al. (2018) [14] | ROC-AUC was very good. Dataset was large. | No comparison in terms of accuracy, precision, and recall. No comparative study was done. |

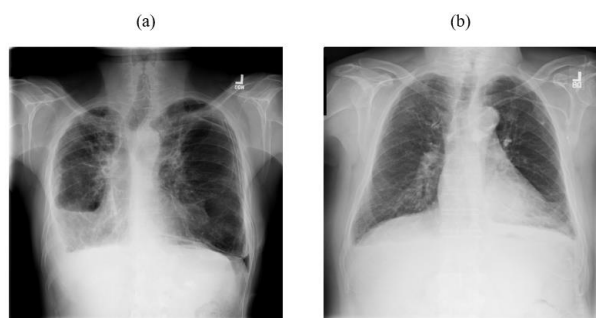


FIGURE 1. Sample of CXR image from original dataset.

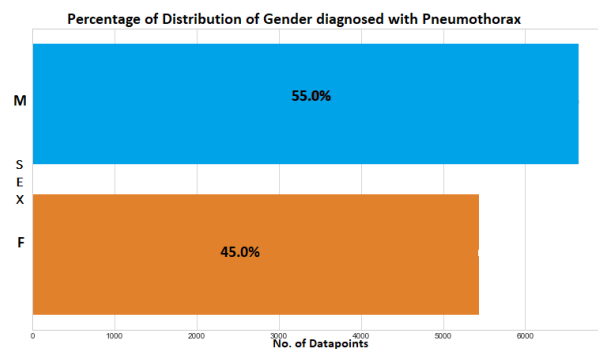


FIGURE 3. Distribution of pneumothorax patients based on gender.

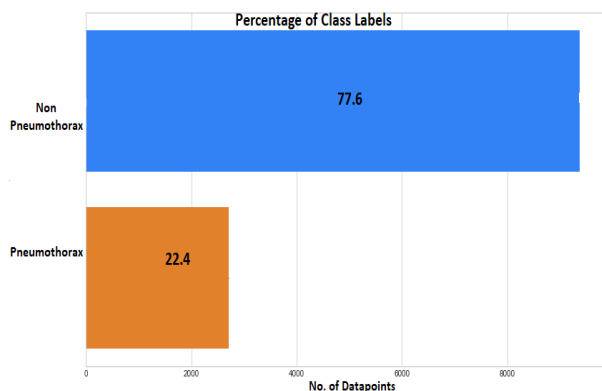


FIGURE 2. Graphical representation of class labels.

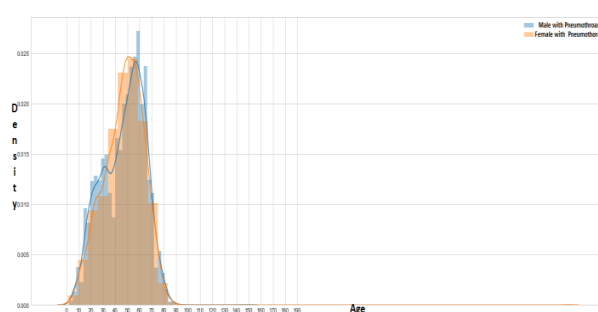


FIGURE 4. Comparative graph between males and females suffering from pneumothorax with their age.

shows the distribution of pneumothorax disease based on gender. According to the graph, 55% of pneumothorax patients were male while the rest 45% were females. So as per the graph, we can observe males were majorly suffering from pneumothorax.

Figure 4 shows the comparative graph between males and females suffering from pneumothorax with their age graph. From the graph, we can notice that the age group between 55-60 is highly impacted by this disastrous pneumothorax.

From Figure 5, it is evident that the age of 58 is highly impacted with pneumothorax where more than 200+ records

are registered and it has been followed by the 175+ cases which are registered at the age of 65. Hence, based on the histogram, it can be concluded that the age group of 50-65 is highly affected by pneumothorax. Additionally, the histogram reveals a notable case where a baby was affected with pneumothorax at the age of 3. Subsequently, there is a substantial shift in the histogram after the age of 15, indicating a drastic increase in pneumothorax cases. Various useful insights can be observed from these visualizations.

C. DATA AUGMENTATION AND PREPROCESSING

Data augmentation plays a crucial role in addressing the issue of imbalanced classes by providing a means to balance the

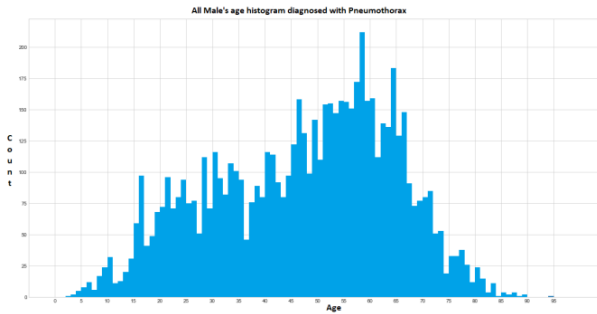


FIGURE 5. Male's age histogram concerning pneumothorax.

distribution of data. It helps by providing various aspects of the sample image by transforming the various properties related to the image. In our case, we can observe from Figure 2 that the dataset was highly imbalanced. From Figure 2 we can observe that 9378 (77.6%) were from the non-pneumothorax class and the rest 2711 (22.4%) were from pneumothorax this shows the highly imbalanced nature of class labels. So for balancing the dataset, Data augmentation played an important role. Data augmentation helps us in regenerating the images from the true images by implementing various parameters like shearing, brightness increment, zooming, shifting, rotating, whitening, cropping, and flipping Data augmentation will lead us to develop a fine-tuned unbiased deep learning architecture. For our approach, Table 2 shows the various parameters used for data augmentation.

TABLE 2. Parameters used for data augmentation.

| Parameters | Values |
|--------------------|------------|
| Rotation range | 10 |
| Width shift range | 0.1 |
| Height shift range | 0.1 |
| Shear range | 0.1 |
| Brightness range | (0.4, 1.0) |
| Horizontal flip | True |
| Vertical flip | True |
| Fill mode | Nearest |

In terms of pre-processing, as images are in the form of DICOM so for a better classification model we have converted the DICOM files into .jpg format for creating the training, testing, and validation set for classification architectures. Table 3 shows the dataset distribution after dataset augmentation. Figure 6 shows the proposed workflow for the classification of pneumothorax using Convolutional Neural Network and Transfer Learning Models.

D. CONVOLUTIONAL NEURAL NETWORK

Convolutional Neural networks (CNN) are a major contributor to imagery data. CNN architectures contribute on large scale towards the day to day applications such as Classification of Skin Cancer lesions [31], [32], Detection and Classification of Mycobacterium Tuberculosis using Convolutional Neural Network [33], [34], Diabetes Disease

TABLE 3. Dataset distribution after image augmentation.

| | Pneumothorax | | Non-Pneumothorax | | Total |
|----------------|---------------|----------------|------------------|----------------|-------|
| | No. of Images | Percentage (%) | No. of Images | Percentage (%) | |
| Training Set | 8544 | 53.24 | 7503 | 46.75 | 16047 |
| Testing Set | 1601 | 46.04 | 1876 | 53.95 | 3477 |
| Validation Set | 1601 | 46.04 | 1876 | 53.95 | 3477 |

Classification using Deep Neural Network [35], Retinal Disease Classification using Optical Coherence Tomography Images (OCT Images) [36], [37] and Soil Classification [38]. Convolution Neural networks can perform better on any imagery data in terms of another deep neural network. These architectures are highly related to a pattern associated with images.

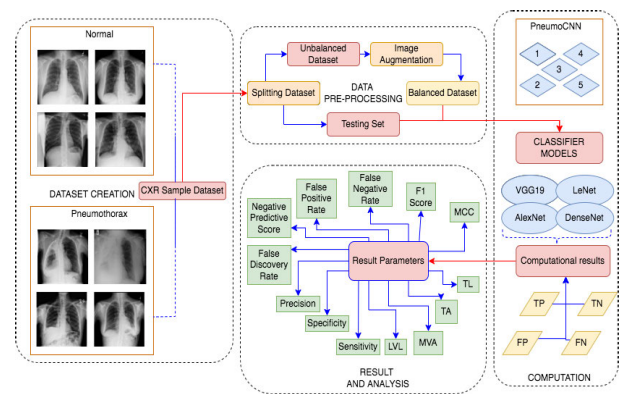


FIGURE 6. Proposed workflow for pneumothorax classification.

This convolutional neural network follows the property of the convolutional theorem and these architectures recognize images through various matrices. In terms of composition, these CNN are composed of four basic layers, 1) Convolutional Layer, 2) Pooling Layer, 3) Flattening and Fully-connected Layer.

1) CONVOLUTIONAL LAYER

This is the primary layer of Convolutional Neural Networks (CNN). The convolutional layer follows the property of the convolutional theorem. Majorly this focuses on the condition where the output of the initial or parent layer acts as the input for the next successive layer. The output received is known as a feature map and these outputs are in the form of vectors. The convolutional theorem is depicted in Equation (1) where x and y are convolutional layers and z refers to the hidden operations.

$$x(y(z)) = y(x(z)) \tag{1}$$

2) POOLING LAYER

Pooling layers are the second basic layer of CNN architectures. These provide us with the facility and help to reduce

the dimensions associated with feature maps. Pooling layers facilitate us by downsampling the feature map by using various spatial variances. Pooling layers can be categorized into two parts: Max-pooling and Average-Pooling. In terms of a mathematical equation, output dimensions can be calculated via Equation (2).

$$Dim_{output} = \frac{(m - f + 1) \times (n - p + 1)}{q(q \times o)} \quad (2)$$

where m represents height (feature map), n represents width (feature map), o represents channel (feature map), p represents the filter size (feature map), and q represents stride length (feature map).

3) FLATTENING LAYER AND FULLY CONNECTED LAYER

The flattening layer is the second last layer of CNN architecture. It plays an important role as it converts the output of the max-pooling layer into a 1-D array which acts as input parameters for the last layer. The fully connected layer is the last layer of CNN architecture and it helps in connecting all the 1-D arrays received through the flattening layer it performs various operations which help to generate various outputs as per requirement.

E. ARTIFICIAL NEURAL NETWORK

Artificial Neural Networks (ANNs) are computational systems inspired by the structure and function of biological neural networks. They simulate the transmission of signals between neurons using a simplified representation of biological nervous systems. ANNs are a subset of machine learning and serve as the foundation for deep learning algorithms. Through self-learning and continuous adjustment of weights and biases, ANNs improve accuracy over time. They are powerful tools for classification, clustering, and pattern recognition tasks. ANNs consist of interconnected nodes, or perceptrons, organized into layers, including input, hidden, and output layers. The input of the processing element, I_n , multiplied by the connection weight, $W_{n,m}$, accelerates the strengthening of neural trails in the network. All the weight-adjusted processing element input are then accumulated through a vector to scalar function via summation which is shown in Equation (3).

$$X = \sum W_{nm} I_n \quad (3)$$

Mathematically, it can be more elaborated as $input \rightarrow y$. Then transform a set $MCBE^y$ of input signals where ($b:y - neuron\ on\ M$) is a function as follows in Equation (4):

$$K : AE^x \times M \ni (\vec{w}, \vec{u}) \rightarrow K(\vec{w}, \vec{u}) = f(\langle \vec{w}, \vec{u} \rangle) \ni BE \quad (4)$$

where, \vec{w} = weight vector; $\langle \dots \rangle$ = real scalar product as follows: $f : BE \rightarrow \beta$

This is known as the activation function of the neuron in Artificial Neural Network layers. If f is a linear operator, then the neuron is linear as follows:

$$K^* := K(\vec{w}, \cdot) : M \ni \vec{u} \rightarrow K^*(\vec{u}) \in BE \quad (5)$$

From Equation (5), K^* is the function known as a model that is trained on the $y - neuron\ on\ M$.

F. TRANSFER LEARNING

Transfer learning is a machine learning method that utilizes knowledge gained from solving related problems and applies it to a different but similar problem. It involves repurposing a pre-trained model to achieve rapid performance on a new problem. Transfer learning saves time and computational resources by reusing pre-trained models instead of training large similar tasks from scratch. It offers advantages such as improved neural network performance and the ability to achieve better accuracy without requiring massive amounts of data.

Domain and tasks can be used as terms for an explanation of transfer learning in a mathematical way.

Let domain Y consist of $S \rightarrow feature\ space$ and $P(D) \rightarrow Marginal\ Probability\ Distribution$ where

$$D = \{s_1, s_2, s_3 \dots \dots \dots s_n\} \in S \quad (6)$$

Let specific domain $Y = \{S, P(D)\}$. It has 2 parts, i.e., $X \rightarrow Label\ Space$ and $\{f : S \rightarrow X\}$ i.e., an objective predictive function.

For new instances, a function f is used for predicting $f(s)$ i.e., the corresponding label.

Now $T = \{X, f(s)\}$ Where T is the task that is learned for the pair i.e., $T\{s_a \in S\} \{x_a \in X\}$ is part of training data $Y_s \rightarrow Source\ domain\ (given)$, $T_s \rightarrow Learning\ task$, $Y_s \rightarrow Target\ domain$, and $T_s \rightarrow Learning\ task$

Where,

$$\begin{aligned} Y_s &\neq Y_t \\ T_s &\neq T_t \end{aligned} \quad (7)$$

where target predictive function $f_s(\cdot)$ T_s, F_s, T_s will be able to improve its learning when transfer learning will be implemented with the help of knowledge in Y_s and T_s .

Transfer learning models are proposed during the ImageNet competition and these architectures outperform all other architectures by gaining very high results and accuracy. In our study we have used 7 transfer learning paradigms for better analysis of pneumothorax classification system. Visual Geometry Group (VGG-19) and Residual Neural Network (ResNet50V2 and ResNet152V2) are widely used architecture among the various transfer learning architectures. Neural Architectural Search Network (NasNetLarge), Densely Connected Convolutional Networks (DenseNet121 and DenseNet201), AlexNet and LeNet are also outstanding paradigms for various deep learning applications. So for better insights and comparative study these architecture played an important for proposing our pneumothorax classification system. Table 4 shows various transfer learning models used in this study:

G. SOFTWARE AND HARDWARE USED

All the implementation was carried out on Jupyter Notebook using Tensorflow (2.8.0) and Keras with Python 3.0.

TABLE 4. Tabular representation of transfer learning models.

| Model Name | Parameters (Million) | Depth |
|-------------|----------------------|-------|
| VGG 19 | 143.7 | 19 |
| NASNetLarge | 88.9 | 533 |
| DenseNet121 | 8.1 | 242 |
| ResNet152V2 | 60.4 | 307 |
| ResNet50V2 | 25.6 | 103 |
| DenseNet201 | 20.2 | 402 |
| AlexNet | 24.7 | 8 |
| LeNet | 6.3 | 7 |

The hardware setup consisted of 16 GB RAM and an i5 8th generation processor. The architectures were saved in .hdf5 format.

IV. RESULTS

This section includes the results and analysis associated with our study. This section comprises 4 sections **IV-A.** Analysis of Pneumo-Convolutional Neural Networks (PneumoCNNs), **IV-B.** Analysis of Transfer Learning Models **IV-C.** Comparison of Transfer Learning Model versus CNNs.

A. ANALYSIS OF PNEUMO-CONVOLUTIONAL NEURAL NETWORKS (PNEUMOCNNs)

In total 7 proposed convolutional neural networks were analysed for classification of pneumothorax using CXR images. Various hyper parameter tunings such as the number of convolutional layers (CL), artificial layer (AL), features detected (FD), input image size (IS), optimizer learning rate, pooling size (PS), kernel size (KS), regularization conditions like L1 and L2, Batch Normalization (BN), and dropout (DO) were considered for the formation of all the CNN architectures. Table 5 shows the configuration for all the proposed Convolutional Neural Networks. Models evaluations were based on different criteria such as Training Time(TT), Normalized Training Time(NormalizedTT), Maximum Validation Accuracy (MVA), Testing Accuracy (TA), Testing Loss (TL), Least Validation Loss (LVL), Sensitivity (Se), Specificity (Sp), F1 Score (F1), Precision (Pr), Negative Predictive Score (NPS), and Matthews Correlation Coefficient (MCC).

PneumoCNN-1 was consisting of 3 convolutional layers and 4 artificial layers which was lightest among all the proposed architectures and it also achieved an accuracy of 0.9883 with very less validation loss of 0.0397. In terms of MVA, the highest validation accuracy was achieved by PneumoCNN-5 of 0.9947 with the LVL of 0.0264 which is very low. This architecture had minimal loss as per the study. But in terms of TA, PneumoCNN-5 was the second-highest scorer. PneumoCNN-5 contained six CL layers and nine AL layers. According to the study, the lowest MVA was achieved by PneumoCNN-6 of 0.9659 due to an imbalance in layers. PneumoCNN-6 consisted of four convolutional layers and eight artificial layers. In terms of weight adjustment,

PneumoCNN-6 was biased towards artificial layers. In terms of LVL, PneumoCNN-6 had a loss of 0.1219 which was very high when compared with all other PneumoCNN architectures.

PneumoCNN-2 scores an MVA of 0.9904 and has a loss of 0.0389 which indicates that light architectures can perform better than heavy configure PneumoCNNs. It is noticed that training time increased concerning layers indulged during the training of neural networks. So we can state that training time is directly proportional to the depth of PneumoCNN. As parameters increased in PneumoCNN through the increment in the number of layers, the models are trying to overfit. So to avoid overfitting, L1, L2, Batch Normalization, and Dropouts have been included. For further consideration, we also configure the learning rate of optimizers. PneumoCNN-4 had optimal performance in all the performance metrics where it had 5 convolutional layers and 7 artificial layers and they helped PneumoCNN-4 to gain the testing accuracy of 0.9008 with the testing loss of 0.1978.

From Table 6, in terms of sensitivity PneumoCNN-7 has the highest scorer with metrics of 0.8864 which is pretty good for any binary classification problem but it has the only score of 0.9488 in terms of specificity. PneumoCNN-2 outperforms all other architectures in terms of specificity by achieving a score of 0.9836 whereas PneumoCNN-6 has the least specificity score of 0.8904. All other architectures achieved a specificity above 0.95. F1 score is a majorly focused performance metric and our PneumoCNNs outperformed in this domain as 5 PneumoCNN achieved an F1 score of 0.90 or above. PneumoCNN-5 had the highest F1 score of 0.9230. In terms of precision, PneumoCNN-2 has the highest score of 0.9888 which is very high, and the lowest score achieved in the field of precision is 0.9163 by PneumoCNN-6. Matthews Correlation Coefficient (MCC) score of 0.8256 was achieved by PneumoCNN-7 and the least MCC was 0.7223 which was achieved by PneumoCNN-6. In terms of Negative Predictive Score (NPS), PneumoCNN7 achieved a value of 0.8557 whereas the lowest NPS was by PneumoCNN-3 which scored just the NPS of 0.7545. Figure 7 shows the performance metrics of all the PeumoCNNs in graphical form.

So for more analysis, Table 7 shows the testing accuracy and testing loss with a confusion matrix for deep analysis. In terms of inference, PneumoCNN-7 outperforms all other PneumoCNN architectures by achieving the highest testing accuracy of 0.9123 and also has a minimal testing loss of 0.1742. In Table 7, it is noticed that PneumoCNN-6 has the lowest scorer at the time of inference where a score of 0.8614 is achieved.

It also has a maximum testing loss of 0.3167 which suggests that after building good relations with the dataset still, PneumoCNN lacks quality inferencing as per scores. So for further consideration, PneumoCNN-7 and PneumoCNN-5 are considered to be the best and optimal architecture for the classification of pneumothorax in various aspects of performance metrics. So, for further consideration PneumoCNN-5

TABLE 5. Configuration of proposed convolutional neural network.

| S.no. | Name | CL | AL | Regularization | | | | IS | FD | KS | PS |
|-------|-------------|----|----|----------------|----|----|----|-----------|------------------------|---------------|---------------|
| | | | | L1 | L2 | BN | DO | | | | |
| 1 | PneumoCNN-1 | 3 | 4 | ✗ | ✗ | ✓ | ✓ | (128,128) | {128,64,32} | {3,3,3} | {2,2,2} |
| 2 | PneumoCNN-2 | 4 | 5 | ✗ | ✗ | ✓ | ✓ | (128,128) | {128,128,64,32} | {3,3,3,3} | {2,2,2,2} |
| 3 | PneumoCNN-3 | 4 | 6 | ✗ | ✗ | ✓ | ✓ | (128,128) | {256,128,64,32} | {3,3,3,3} | {2,2,2,2} |
| 4 | PneumoCNN-4 | 5 | 7 | ✓ | ✓ | ✓ | ✓ | (128,128) | {256,128,64,32,32} | {6,6,6,3,3} | {2,2,2,2,2} |
| 5 | PneumoCNN-5 | 6 | 9 | ✓ | ✓ | ✓ | ✓ | (128,128) | {256,128,64,64,32,16} | {3,3,3,3,3,3} | {2,2,2,2,2,2} |
| 6 | PneumoCNN-6 | 4 | 8 | ✗ | ✗ | ✗ | ✗ | (128,128) | {512,256,128,64} | {6,6,3,3} | {4,2,2,2} |
| 7 | PneumoCNN-7 | 6 | 10 | ✓ | ✓ | ✓ | ✓ | (128,128) | {256,128,128,64,32,16} | {3,3,3,3,3,3} | {2,2,2,2,2,2} |

TABLE 6. Performance metrics of PneumoCNN architectures.

| Model Name | MVA | LVL | Sc | Sp | F1 | Pr | NPS | TT (in seconds) | MCC |
|-------------|--------|--------|--------|--------|--------|--------|--------|-----------------|--------|
| PneumoCNN-1 | 0.9883 | 0.0397 | 0.8351 | 0.9786 | 0.9042 | 0.9856 | 0.7720 | 11213 | 0.7852 |
| PneumoCNN-2 | 0.9904 | 0.0389 | 0.8451 | 0.9836 | 0.9113 | 0.9888 | 0.7876 | 14092 | 0.8022 |
| PneumoCNN-3 | 0.9830 | 0.0891 | 0.8244 | 0.9750 | 0.8969 | 0.9835 | 0.7545 | 24494 | 0.7681 |
| PneumoCNN-4 | 0.9883 | 0.0572 | 0.8616 | 0.9618 | 0.9136 | 0.9723 | 0.8170 | 4480 | 0.8061 |
| PneumoCNN-5 | 0.9947 | 0.0264 | 0.8663 | 0.9828 | 0.9230 | 0.9877 | 0.8214 | 4592 | 0.8289 |
| PneumoCNN-6 | 0.9659 | 0.1219 | 0.8410 | 0.8904 | 0.8770 | 0.9163 | 0.7970 | 19245 | 0.7223 |
| PneumoCNN-7 | 0.9856 | 0.0628 | 0.8864 | 0.9488 | 0.9220 | 0.9606 | 0.8557 | 4349 | 0.8256 |

TABLE 7. Testing results, normalized training time, and confusion matrix concerning PneumoCNN architectures.

| Model Name | NormalizedTT | TA | TL | Confusion Matrix | |
|-------------|--------------|--------|--------|------------------|------|
| PneumoCNN-1 | 0.2623 | 0.8872 | 0.2975 | 1849 | 27 |
| PneumoCNN-2 | 0.3723 | 0.8961 | 0.2432 | 365 | 1236 |
| PneumoCNN-3 | 0.7698 | 0.8781 | 0.2355 | 1855 | 21 |
| PneumoCNN-4 | 0.0050 | 0.9008 | 0.1978 | 340 | 1261 |
| PneumoCNN-5 | 0.0092 | 0.9111 | 0.2098 | 1845 | 31 |
| PneumoCNN-6 | 0.5692 | 0.8614 | 0.3167 | 393 | 1208 |
| PneumoCNN-7 | 0.0000 | 0.9123 | 0.1742 | 1824 | 52 |
| | | | | 293 | 1308 |
| | | | | 1853 | 23 |
| | | | | 286 | 1315 |
| | | | | 1719 | 157 |
| | | | | 325 | 1276 |
| | | | | 1802 | 74 |
| | | | | 231 | 1370 |

is referred to as PneuNetV0, and PneumoCNN-7 is referred to as PneuNetV1.

B. ANALYSIS OF TRANSFER LEARNING MODELS

In terms of transfer learning model, in total seven models are considered namely, VGG-19, NASNetLarge, DenseNet121, ResNet152V2, DenseNet201, AlexNet, LeNet. All transfer learning models are enriched in parameters and have been trained on the pneumothorax dataset by using Keras and TensorFlow. In terms of computational cost, these architectures are very complex due to their large training time.

During inference and testing, these models are lagging behind our PneumoCNN models.

For better analysis and result gathering, transfer learning models have been compared in terms of performance metrics in Table 8. VGG-19 dominates in almost every performance metric. VGG-19 has the highest specificity of 0.8829, the highest F1 score of 0.9293, the highest negative predictive score of 0.8476, and the MCC score of 0.8426. NASNetLarge has the lowest scores of 0.7031 and 0.5522 in sensitivity and negative predictive, respectively. ResNet50V2 scores very less in specificity, precision, MCC, and F1 with a score of

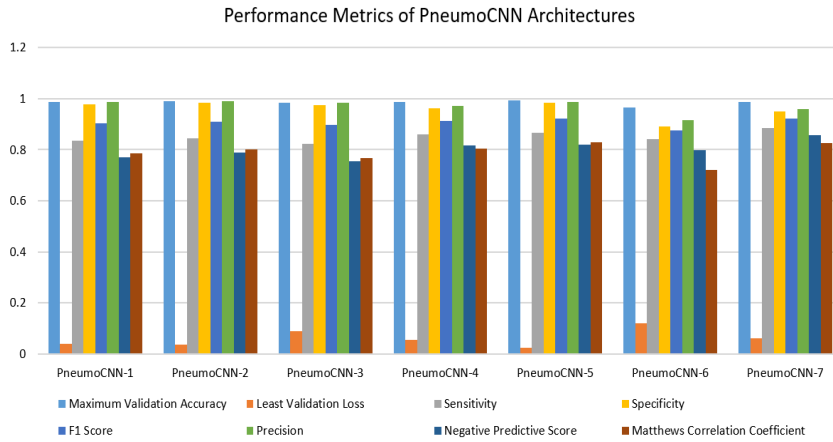


FIGURE 7. Performance metrics of PneuMoCNN architectures.

TABLE 8. Performance metrics of transfer learning architectures.

| Model Name | MVA | LVL | Sc | Sp | F1 | Pr | NPS | TT | MCC |
|-------------|--------|--------|--------|--------|--------|--------|--------|--------------|--------|
| | | | | | | | | (in seconds) | |
| VGG-19 | 0.9963 | 0.0199 | 0.8829 | 0.9742 | 0.9293 | 0.9808 | 0.8476 | 23389 | 0.8426 |
| NASNetLarge | 0.9009 | 0.5882 | 0.7031 | 0.8324 | 0.7914 | 0.9051 | 0.5522 | 30515 | 0.4948 |
| DenseNet121 | 0.7933 | 0.5137 | 0.8097 | 0.7637 | 0.8016 | 0.7937 | 0.7814 | 8643 | 0.5743 |
| ResNet152V2 | 0.8583 | 0.5048 | 0.7071 | 0.7812 | 0.7764 | 0.8600 | 0.5821 | 17241 | 0.4651 |
| ResNet50V2 | 0.7906 | 0.5817 | 0.7247 | 0.7284 | 0.7579 | 0.7942 | 0.6465 | 8874 | 0.4468 |
| DenseNet201 | 0.8737 | 0.4505 | 0.7388 | 0.7884 | 0.7913 | 0.8518 | 0.6471 | 15984 | 0.5129 |
| AlexNet | 0.9984 | 0.0100 | 0.7764 | 0.9861 | 0.8711 | 0.9920 | 0.6852 | 8244 | 0.7079 |
| LeNet | 0.9995 | 0.6263 | -- | 0.4605 | 0.0000 | 0.0000 | 1.0000 | 4445 | -- |

TABLE 9. Testing results, normalized training time, and confusion matrix concerning transfer learning models.

| Model Name | Normalized TT | TA | TL | Confusion Matrix | |
|-------------|---------------|--------|--------|------------------|------|
| VGG19 | 0.7276 | 0.9194 | 0.1968 | 1840 | 36 |
| | | | | 244 | 1357 |
| NASNetLarge | 1.0000 | 0.7425 | 0.2801 | 1698 | 178 |
| | | | | 717 | 884 |
| DenseNet121 | 0.1641 | 0.7880 | 0.2693 | 1489 | 387 |
| | | | | 350 | 1251 |
| ResNet152V2 | 0.4927 | 0.7325 | 0.3592 | 1615 | 261 |
| | | | | 669 | 932 |
| ResNet50V2 | 0.1729 | 0.7262 | 0.3518 | 1490 | 386 |
| | | | | 566 | 1035 |
| DenseNet201 | 0.4446 | 0.7575 | 0.2880 | 1598 | 278 |
| | | | | 565 | 1036 |
| AlexNet | 0.1488 | 0.8415 | 0.2174 | 1861 | 15 |
| | | | | 536 | 1065 |
| LeNet | 0.0036 | 0.4605 | 0.8923 | 0 | 1876 |
| | | | | 0 | 1601 |

0.7284, 0.7942, 0.4468, and 0.7579 respectively. So we can state that ResNet50V2 was not a good performer at all and had the least connections with the dataset. LeNet has been the worst performer as it is overfitted with the dataset. LeNet has a very weak relationship with the dataset where positive

classes are not identified and architecture is inclined towards only one class. During training, LeNet achieves an accuracy of 0.9995 but it is overfitted and the results are not good. So in terms of consideration, LeNet cannot be considered as an architecture for comparison.

Performance Metrics of Transfer Learning Models

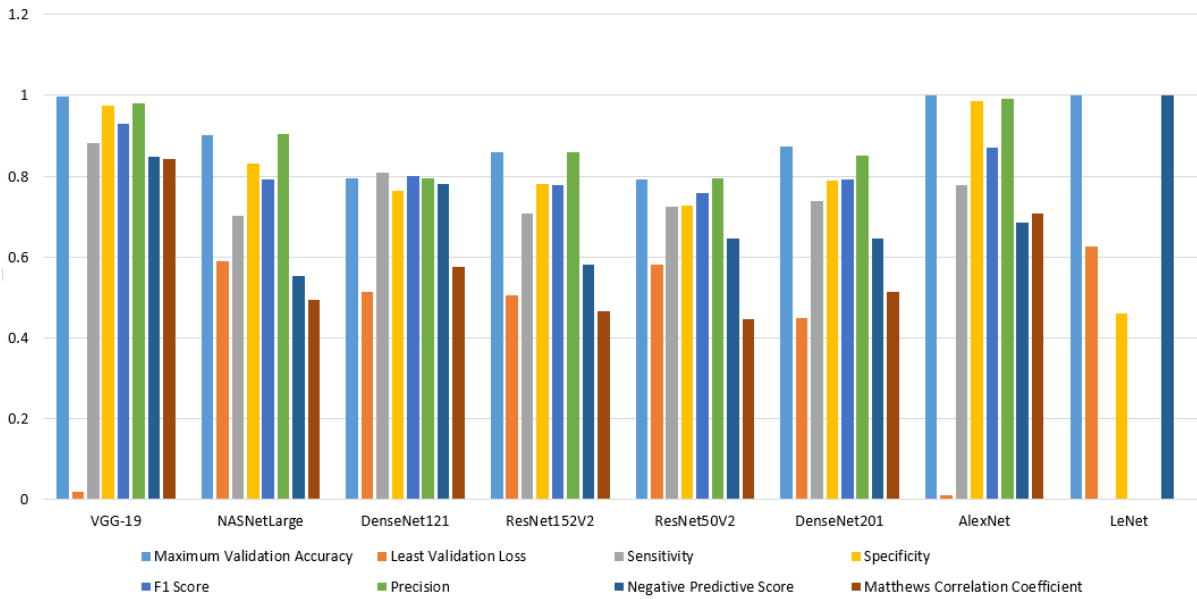


FIGURE 8. Performance metrics of transfer learning.

TABLE 10. Performance metrics of selected models.

| Performance Criteria | PneuNetV0 | | PneuNetV1 | | VGG-19 | |
|---------------------------|-----------|------|-----------|------|--------|------|
| MVA | 0.9947 | | 0.9856 | | 0.9963 | |
| LVL | 0.0264 | | 0.0628 | | 0.0199 | |
| TA | 0.9111 | | 0.9123 | | 0.9194 | |
| TL | 0.2098 | | 0.1742 | | 0.1968 | |
| Sensitivity | 0.8663 | | 0.8864 | | 0.8829 | |
| Specificity | 0.9828 | | 0.9488 | | 0.9742 | |
| Precision | 0.9877 | | 0.9606 | | 0.9808 | |
| Negative Predictive Score | 0.8214 | | 0.8557 | | 0.8476 | |
| False Positive Rate | 0.0172 | | 0.0512 | | 0.0258 | |
| False Discovery Rate | 0.0123 | | 0.0394 | | 0.0192 | |
| False Negative rate | 0.1337 | | 0.1136 | | 0.1171 | |
| F1 Score | 0.9230 | | 0.9220 | | 0.9293 | |
| Efficacy Score | 4.1602 | | 5.2370 | | 0.9945 | |
| MCC | 0.8289 | | 0.8256 | | 0.8426 | |
| Confusion Matrix | 1853 | 23 | 1802 | 74 | 1840 | 36 |
| | 286 | 1315 | 231 | 1370 | 244 | 1357 |

From Table 9, it is noticed that VGG-19 has the best classifier for pneumothorax in terms of transfer learning models with a testing accuracy of 0.9194 and also has a minimal loss of 0.1968. Figure 8 shows the performance metrics of the transfer learning model. So for further consideration, VGG 19 is considered the best transfer learning model.

C. COMPARISON OF TRANSFER LEARNING MODELS VERSUS SELECTED PNEUNET

PneuNetV0 and PneuNetV1 are considered to be the best classification architecture among all PneumoCNN models. In transfer learning, VGG-19 is considered to be the best and optimal model in the transfer learning category. Table 10 shows a detailed comparison of all the three selected

architectures for classification and Figure 9 shows the graphical comparison of selected models. For proposing an efficient architecture, the efficiency ratio is considered to be the most important factor. Equation (8) shows the mathematical formula for the calculation of the efficacy score.

$$Efficacy\ Score = \frac{Testing\ Accuracy}{Testing\ Loss + Normalized\ Training\ Time} \quad (8)$$

From table 10, we can observe that in terms of MVA VGG-19 scored the highest by gaining an MVA of 0.9963 whereas it also had minimal LVL. For accurate testing, VGG 19 dominated by gaining the testing accuracy (TA) of 0.9194. In terms of TL, PneuNetV1 had minimal TL with a score of 0.1742.

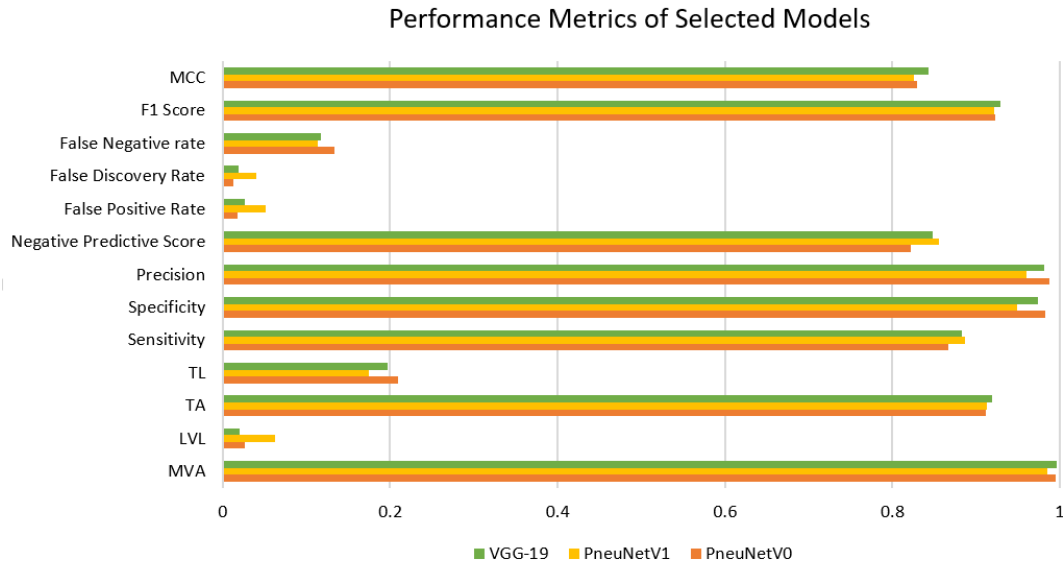


FIGURE 9. Performance metrics of selected models.

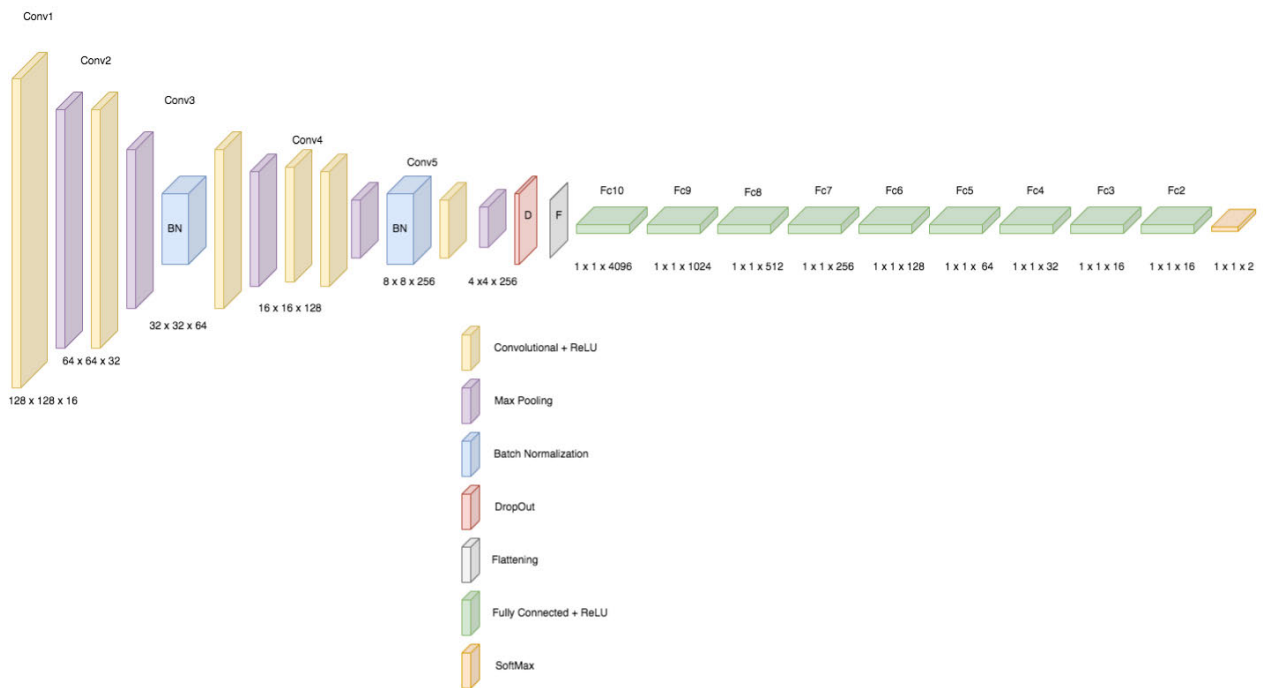


FIGURE 10. Structural view of PneuNetV1.

In terms of specificity and precision, PneuNetV0 outperformed the other two models. While looking into an important ratio factor, we have noticed that PneuNetV1 is the least complex, and the results gained by PneuNetV1 are good with a low computational cost. PneuNetV1 has an efficiency ratio of 5.237 which implies that this architecture can work with a low computational cost and will work as a feasible tool for various medical specialists and physicians. From Figure 9 we

can state that PneuNetV1 performed best in terms of all the performance metrics.

V. DISCUSSION

PneuNetV1 is an efficient architecture for the classification of Pneumothorax. Pneumothorax is a critical collapsed lung condition that can lead to severe consequences. So to overcome the classification of CXR images of Pneumothorax,

TABLE 11. Comparison with related work.

| Author Name | No. of Pneumothorax Images used for training | Accuracy | Precision | Sensitivity | Specificity |
|--------------------|---|---------------|---------------|---------------|---------------|
| Chan et al. [15] | 22 | 0.8580 | 0.8360 | 0.8740 | -- |
| Li et al. [17] | 50 | -- | -- | 1.0000 | 0.8250 |
| Taylor et al. [18] | 3107 | -- | -- | 0.8400 | 0.9000 |
| PneuNetV1 | 8544 | 0.9123 | 0.9606 | 0.8864 | 0.9488 |

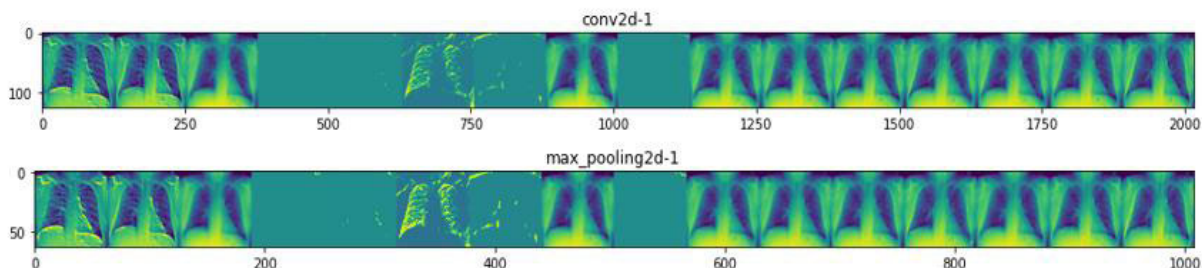


FIGURE 11. Neural activation of PneuNetV1 (first convolutional layers).

we have proposed an efficient deep learning architecture. PneuNetV1 consisted of six convolutional layers with ten artificial layers. Figure 10 provides the structural view of PneuNetV1. PneuNetV1 has the least training time and the model is fully trained on the Pneumothorax dataset by 4349 seconds. Maximum validation accuracy achieved by PneuNetV1 was found to be 0.9856 while testing accuracy is 0.9123 which is very high.

PneuNetV1 outperformed all the other proposed works by gaining the accuracy of 0.9123 with less training time. This study proposed a paradigm which is an efficient tool with low computational cost as this architecture can be easily deployed on classification system machines and portals for an accurate result in less time. As training was based on 8544 positive test of pneumothorax which resulted in an better training of paradigm for the classification of pneumothorax cases when compared with all other previous studies. PneuNetV1 is a light weight CNN paradigm which can be easily trained further on more datasets as per current training report we state that for training of this paradigm on 16047 CXR images it took 4349 seconds so this state of the art architecture can also outperform all the other proposed architectures by training almost 4 images per second.

In terms of loss of PneuNetV1, the least validation loss and testing loss were found to be 0.0628 and 0.1742 respectively. These all performance metrics led to high efficacy score of 5.2370. In terms of F1 score, PneuNetV1 had a score of 0.9220. So PneuNetV1 was highly balanced in performance metrics with an efficient training time. PneuNetV1 was trained on 8544 images. PneuNetV1 is a light weighted paradigm when compared with transfer learning models. So due to its light weighted nature PneuNetV1 can be easy retrained on new datasets and can act as a real world

deployed classification system which can be handled at low cost maintenance and raining cost. PneuNetV1 was trained on 8544 pneumothorax cases which helped the model for a better understanding regarding the pneumothorax region for better classification. PneuNetV1 can be a feasible tool for pneumothorax classification by the real world deployment of this paradigms for clinical purpose which can beneficial for physicians and medical experts for a quick classification of pneumothorax patients though Chest X-ray images.

While comparing the size of positive cases in the training set, images used in other related work are less in number for training when compared with our dataset. In terms of results, Chan et al. [15] had less precision and sensitivity than our proposed work. They did not provide the specificity of their best model. Li et al. [17] and Taylor et al. [18] provided and compared their results in terms of Sensitivity and Specificity. Chan et al. [15] gained the accuracy, precision and sensitivity of 0.8587, 0.8360 and 0.8740 but results of PneuNetV1 outperformed results of Chan et al. in terms of all performance metrics calculated. Li et al. [17] and Taylor et al. [18] calculated results on the basis of sensitivity and specificity where Li et al. [17] gained sensitivity and specificity of 1.000 and 0.8250 respectively. Similarly, Taylor at al. [18] gained sensitivity of 0.8400 and specificity 0.9000 but PneuNetV1 gained highest specificity of 0.9488 among all the related works. In terms of sensitivity, Li et al. [17] outperformed PneuNetV1 but they had less training images and they also lacked in all other performance metrics. Overall PneuNetV1 is an optimal architecture for a pneumothorax classification system as it was evaluated on all the performance metrics with Efficacy Score and it also outperformed all the existing studies. Table 11 shows the comparison of our work with other related and reported best works. PneuNetV1

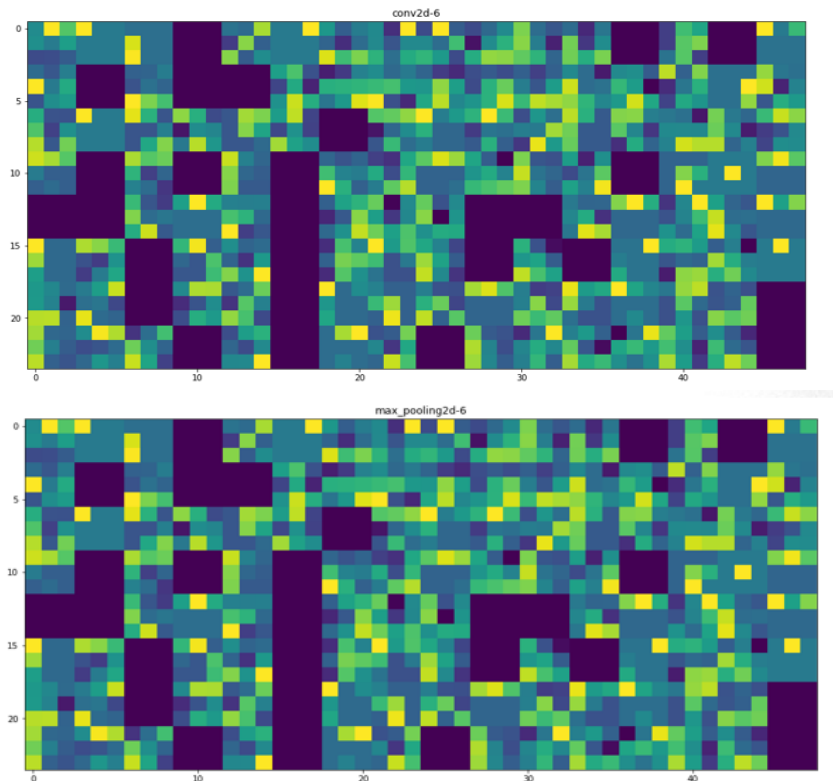


FIGURE 12. Neural activation of PneuNetV1 (last convolutional layers).

has performed excellently by outperforming all the state-of-the-art architectures. To the best of our knowledge, we can claim that the proposed PneuNetV1 is the most efficient Pneumothorax classification model with low computational costs.

Neural activation heatmap provides the better insights regarding the background working of PneuNetV1. Figure 11, Figure 12, shows the neural activation of first and last convolutional layers present in PneuNetV1.

VI. CONCLUSION AND FUTURE WORK

Here, the main focus is to develop a lightweight CNN model that can classify Pneumothorax from CXR images. Lightweight CNN signifies less trainable parameters, training, and inference time. In biomedical image classification, the correctness of the model is very important. The deep learning-based proposed PneuNetV1 provides the best performance over popular SOTA CNN models. It reaches higher accuracy and achieves better results than the existing methods in this domain. In this work, an optimal approach for the classification of pneumothorax is proposed by considering low computational cost as an important factor where training time and efficacy ratio are considered for the selection of optimal architecture. PneuNetV1 is the most optimal architecture for the classification of Pneumothorax CXR images by gaining an efficacy score of 5.2370, testing accuracy of 0.9220, and training time of 4349 seconds (minimum among the fourteen

used models). Furthermore, it is observed that a light architecture performs better in less training time when compared with heavy architectures.

In the future, PneuNetV1 will be compared with other models such as EfficientNet and MobileNet variants for the classification task. Classification indicates the detection of Pneumothorax, but the localization of the infected region of the lungs is missing. Semantic segmentation can be a possible solution to pinpoint the area of interest. We have already started working in the direction of developing a PneuNetV1 encoder-based UNet architecture for efficient semantic segmentation.

ACKNOWLEDGMENT

The author would like to acknowledge and thank all the coauthors for their kind support all the times.

REFERENCES

- [1] Picture of the Lungs. *WebMD*. Accessed: Mar. 21, 2022. [Online]. Available: <https://www.webmd.com/lung/ss/slideshow-lung-facts-overview>
- [2] M. K. Gourisaria, G. Jee, G. M. Harshvardhan, V. Singh, P. K. Singh, and T. C. Workneh, "Data science appositeness in diabetes mellitus diagnosis for healthcare systems of developing nations," *IET Commun.*, vol. 16, no. 5, pp. 532–547, Mar. 2022.
- [3] H. Das, B. Naik, and H. S. Behera, "Classification of diabetes mellitus disease (DMD): A data mining (DM) approach," in *Progress in Computing, Analytics and Networking*. Singapore: Springer, 2018, pp. 539–549.
- [4] Q. Wang, D. Yang, Z. Li, X. Zhang, and C. Liu, "Deep regression via multi-channel multi-modal learning for pneumonia screening," *IEEE Access*, vol. 8, pp. 78530–78541, 2020.

- [5] M. K. Gourisaria, G. M. Harshvardhan, R. Agrawal, S. S. Patra, S. S. Rautaray, and M. Pandey, "Arrhythmia detection using deep belief network extracted features from ECG signals," *Int. J. E-Health Med. Commun.*, vol. 12, no. 6, pp. 1–24, Jul. 2021.
- [6] S. Murugan, C. Venkatesan, M. G. Sumithra, X. Gao, B. Elakkiya, M. Akila, and S. Manoharan, "DEMNET: A deep learning model for early diagnosis of Alzheimer diseases and dementia from MR images," *IEEE Access*, vol. 9, pp. 90319–90329, 2021.
- [7] V. Singh, M. K. Gourisaria, and H. Das, "Performance analysis of machine learning algorithms for prediction of liver disease," in *Proc. IEEE 4th Int. Conf. Comput., Power Commun. Technol. (GUCON)*, Sep. 2021, pp. 1–7.
- [8] M. A. Salam, S. Taha, and M. Ramadan, "COVID-19 detection using federated machine learning," *PLoS ONE*, vol. 16, no. 6, Jun. 2021, Art. no. e0252573.
- [9] I. Saha, M. K. Gourisaria, and G. M. Harshvardhan, "Classification system for prediction of chronic kidney disease using data mining techniques," in *Advances in Data and Information Sciences*. Singapore: Springer, 2022, pp. 429–443.
- [10] R. Chatterjee, A. Chatterjee, and R. Halder, "An efficient pneumonia detection from the chest X-ray images," in *Proc. Int. Conf. Mach. Intell. Data Science Appl.* Singapore: Springer, 2021, pp. 779–789.
- [11] A. Craik, Y. He, and J. L. Contreras-Vidal, "Deep learning for electroencephalogram (EEG) classification tasks: A review," *J. Neural Eng.*, vol. 16, no. 3, Jun. 2019, Art. no. 031001.
- [12] R. Chatterjee, T. Maitra, S. H. Islam, M. M. Hassan, A. Alamri, and G. Fortino, "A novel machine learning based feature selection for motor imagery EEG signal classification in Internet of Medical Things environment," *Future Gener. Comput. Syst.*, vol. 98, pp. 419–434, Sep. 2019.
- [13] H. Das, B. Naik, and H. S. Behera, "An experimental analysis of machine learning classification algorithms on biomedical data," in *Proc. 2nd Int. Conf. Commun. Devices Comput.*, 2020, pp. 525–539.
- [14] G. Kitamura and C. Deible, "Retraining an open-source pneumothorax detecting machine learning algorithm for improved performance to medical images," *Clin. Imag.*, vol. 61, pp. 15–19, May 2020.
- [15] Y. H. Chan, Y. Z. Zeng, H. C. Wu, M. C. Wu, and H. M. Sun, "Effective pneumothorax detection for chest X-ray images using local binary pattern and support vector machine," *J. Healthc. Eng.*, vol. 2018, pp. 1–8, Dec. 2018.
- [16] S. Röhrich, T. Schlegl, C. Bardach, H. Prosch, and G. Langs, "Deep learning detection and quantification of pneumothorax in heterogeneous routine chest computed tomography," *Eur. Radiol. Exp.*, vol. 4, no. 1, pp. 1–11, Dec. 2020.
- [17] X. Li, J. H. Thrall, S. R. Digumarthy, M. K. Kalra, P. V. Pandharipande, B. Zhang, C. Nitiwarangkul, R. Singh, R. D. Khera, and Q. Li, "Deep learning-enabled system for rapid pneumothorax screening on chest CT," *Eur. J. Radiol.*, vol. 120, Nov. 2019, Art. no. 108692.
- [18] A. G. Taylor, C. Mielke, and J. Mongan, "Automated detection of moderate and large pneumothorax on frontal chest X-rays using deep convolutional neural networks: A retrospective study," *PLOS Med.*, vol. 15, no. 11, Nov. 2018, Art. no. e1002697.
- [19] T. Lindsey, R. Lee, R. Grisell, S. Vega, and S. Veazey, "Automated pneumothorax diagnosis using deep neural networks," in *Proc. Iberoam. Congr. Pattern Recognit.*, 2018, pp. 723–731.
- [20] S. Chandra, M. K. Gourisaria, G. M. Harshvardhan, D. Konar, X. Gao, T. Wang, and M. Xu, "Prolificacy assessment of spermatozoan via state-of-the-art deep learning frameworks," *IEEE Access*, vol. 10, pp. 13715–13727, 2022.
- [21] J. S. Almeida, P. P. R. Filho, T. Carneiro, W. Wei, R. Damaševičius, R. Maskeliūnas, and V. H. C. de Albuquerque, "Detecting Parkinson's disease with sustained phonation and speech signals using machine learning techniques," *IEEE Access*, vol. 7, pp. 148083–148092, 2019.
- [22] V. Singh, M. K. Gourisaria, G. M. Harshvardhan, S. S. Rautaray, M. Pandey, M. Sahni, E. Leon-Castro, and L. F. Espinoza-Audelo, "Diagnosis of intracranial tumors via the selective CNN data modeling technique," *IEEE Access*, vol. 12, pp. 2900–2909, 2022.
- [23] M. A. Kassem, K. M. Hosny, R. Damaševičius, and M. M. Eltoukhy, "Machine learning and deep learning methods for skin lesion classification and diagnosis: A systematic review," *IEEE Access*, vol. 11, pp. 1390–1407, 2021.
- [24] R. Pramanik, S. Khare, G. M. Harshvardhan, and M. K. Gourisaria, "A comparative study for depression prediction using machine learning classification models," in *Advances in Data and Information Sciences*. Singapore: Springer, 2022, pp. 233–246.
- [25] W. Hong, E. J. Hwang, J. H. Lee, J. Park, J. M. Goo, and C. M. Park, "Deep learning for detecting pneumothorax on chest radiographs after needle biopsy: Clinical implementation," *Radiology*, vol. 303, no. 2, pp. 433–441, May 2022.
- [26] C.-C. Lee, C.-S. Lin, C.-S. Tsai, T.-P. Tsao, C.-C. Cheng, J.-T. Liou, W.-S. Lin, C.-C. Lee, J.-T. Chen, and C. Lin, "A deep learning-based system capable of detecting pneumothorax via electrocardiogram," *Eur. J. Trauma Emergency Surgery*, vol. 48, no. 4, pp. 1–10, 2022.
- [27] S. Feng, Q. Liu, A. Patel, S. U. Bazai, C. K. Jin, J. S. Kim, M. Sarrafzadeh, D. Azzollini, J. Yeoh, E. Kim, and S. Gordon, "Automated pneumothorax triaging in chest X-rays in the New Zealand population using deep-learning algorithms," *J. Med. Imag. Radiat. Oncol.*, vol. 66, no. 5, pp. 653–659, 2022.
- [28] Y. Tian, J. Wang, W. Yang, J. Wang, and D. Qian, "Deep multi-instance transfer learning for pneumothorax classification in chest X-ray images," *Med. Phys.*, vol. 49, no. 1, pp. 231–243, Jan. 2022.
- [29] V. D. Kumar, P. Rajesh, O. Geman, M. D. Craciun, M. Arif, and R. Filip, "Quo vadis diagnosis?: Application of informatics in early detection of pneumothorax," *Diagnostics*, vol. 13, no. 7, p. 1305, 2023.
- [30] Kaggle. *SIIM-ACR Pneumothorax Segmentation*. Accessed: Feb. 5, 2022. [Online]. Available: <https://www.kaggle.com/datasets/abhishek/siimdicom-images?select=siim-original>
- [31] M. A. Albahar, "Skin lesion classification using convolutional neural network with novel regularizer," *IEEE Access*, vol. 7, pp. 38306–38313, 2019.
- [32] A. Sannigrahi, V. Singh, M. K. Gourisaria, and R. Srivastava, "Diagnosis of skin cancer using feature engineering techniques," in *Proc. 3rd Int. Conf. Adv. Comput., Commun. Control Netw. (ICAC3N)*, Dec. 2021, pp. 405–411.
- [33] C. Liu, Y. Cao, M. Alcantara, B. Liu, M. Brunette, J. Peinado, and W. Curioso, "TX-CNN: Detecting tuberculosis in chest X-ray images using convolutional neural network," in *Proc. IEEE Int. Conf. Image Process. (ICIP)*, Sep. 2017, pp. 2314–2318.
- [34] V. Singh, M. K. Gourisaria, G. M. Harshvardhan, and V. Singh, "Mycobacterium tuberculosis detection using CNN ranking approach," in *Advanced Computational Paradigms and Hybrid Intelligent Computing*. Singapore: Springer, 2022, pp. 583–596.
- [35] A. K. Sahoo, C. Pradhan, and H. Das, "Performance evaluation of different machine learning methods and deep-learning based convolutional neural network for health decision making," in *Nature Inspired Computing for Data Science*. Cham, Switzerland: Springer, 2020, pp. 201–212.
- [36] A. P. Sunija, S. Kar, S. Gayathri, V. P. Gopi, and P. Palanisamy, "OctNET: A lightweight CNN for retinal disease classification from optical coherence tomography images," *Comput. Methods Programs Biomed.*, vol. 200, Mar. 2021, Art. no. 105877.
- [37] S. Sarah, V. Singh, M. K. Gourisaria, and P. K. Singh, "Retinal disease detection using CNN through optical coherence tomography images," in *Proc. 5th Int. Conf. Inf. Syst. Comput. Netw. (ISCON)*, Oct. 2021, pp. 1–7.
- [38] K. Chatterjee, M. S. Obaidat, D. Samanta, B. Sadoun, S. H. Islam, and R. Chatterjee, "Classification of soil images using convolution neural networks," in *Proc. Int. Conf. Commun., Comput., Cybersecurity, Informat. (CCCI)*, Oct. 2021, pp. 1–5.



MAHENDRA KUMAR GOURISARIA (Member, IEEE) received the master's degree in computer application from Indira Gandhi National Open University, New Delhi, and the M.Tech. degree in computer science and engineering from the Biju Patnaik University of Technology, Rourkela. He is currently pursuing the Ph.D. degree with KIIT Deemed to be University, Bhubaneswar, Odisha. He is an Assistant Professor with the School of Computer Engineering, KIIT Deemed to be University.

He has an experience of more than 19 years in academia and eight years in research. He has guided more than 60 B.Tech. students in their project work and seven M.Tech. thesis. He has published more than 100 research papers in different book chapters, international journals, and conferences of repute. His research interests include cloud computing, machine learning, deep learning, data mining, soft computing, and internet and web technology. He is a member of IAENG and UACEE, and a Life Member of ISTE, CSI, and ISCA. He has served as an organizing committees members for various conferences and workshops.



include the advancement of machine learning and deep learning, artificial intelligence, data pipeline, computer vision, and natural language processing. He has won various medals in quizzes, art, and sports competition at state level.

VINAYAK SINGH is currently pursuing the bachelor's degree with the School of Computer Engineering, KIIT Deemed to be University. He is a Data Engineer with GE HealthCare. He has also completed four internships in field of data science and engineering. He collaborated with Siemens AI Team for a research project. He has published more than 15 research papers in different reputed international journals, conferences, and book chapters with more than 50 citations. His research interests



professor with the School of Computer Engineering, KIIT Deemed to be University. He is also an Expert Member with the Cognitive Systems and Cybernetics Research Laboratory, MIU, ISI. He has published research articles in many reputed international conferences and journals. His research interests include brain-computer interface, machine learning, deep learning, and computer vision. He received the MHRD (Government of India) Scholarship for his master's degree for possessing All India Rank 1410 in GATE-2008. He is a regular Reviewer of various reputed journals, such as *Medical and Biological Engineering and Computing* (SCI-E, IF: 2.602), *IEEE TRANSACTIONS ON BIOMEDICAL ENGINEERING* (SCI-E, IF: 4.538), *IEEE JOURNAL OF BIOMEDICAL AND HEALTH INFORMATICS* (SCI-E, IF: 5.223), *Computers in Biology and Medicine* (SCI-E, IF: 4.589), *IEEE TRANSACTIONS ON EMERGING TOPICS IN COMPUTATIONAL INTELLIGENCE* (Scopus, IF: 8.28), and *Evolutionary Intelligence* (Scopus, DBLP). He is one of the founding members of the international conference series on computational intelligence and networks (<http://www.cineconf.org>).

RAJDEEP CHATTERJEE received the B.E. degree in computer science and engineering from The University of Burdwan, in 2008, and the M.Tech. and Ph.D. degrees in computer science and engineering from KIIT Deemed to be University, Bhubaneswar, India, in 2011 and 2020, respectively. He started his professional career as a Project Linked Person with the Machine Intelligence Unit (MIU), Indian Statistical Institute (ISI), Kolkata, India. He is currently an Associate Pro-



Institute of Information Technology, Design and Manufacturing, Kurnool, Andhra Pradesh, India, and an Assistant Professor with the Department of Information Technology, VSSUT. He is currently an Assistant Professor with the Department of Computer Science and Engineering, NIT Warangal, Telangana, India. He has nine years of teaching and research experience.

SANJAYA KUMAR PANDA (Senior Member, IEEE) received the B.Tech. degree in computer science and engineering from the Veer Surendra Sai University of Technology (VSSUT), Burla, Odisha, India, the M.Tech. degree from the National Institute of Technology (NIT), Rourkela, Odisha, and the Ph.D. degree from IIT (ISM) Dhanbad, Jharkhand, India. He was an Assistant Professor and the Head of the Department of Computer Science and Engineering, Indian

He has guided 30 B.Tech. students, 17 M.Tech./M. Phil./M.C.A. scholars, and two Ph.D. scholars, and guiding five Ph.D. scholars. His Google Scholars citations reached more than 1800 with an H-index of 23 and i10-index of 46. He has published more than 120 papers in reputed journals and conferences, and edited four books. His current research interests include cloud and fog computing, artificial intelligence, machine learning, and the Internet of Things. He is a member of IE(I) and a Life Member of ISTE and CSI. He received 22 awards from IEEE, IE (I), ISTE, CSI, and others, which includes two silver medal awards for the best graduate and best postgraduate in CSE and CSI and ACM distinguished speaker. He is listed in the top 2% of world scientists in a single year impact as per the survey conducted by Stanford University, USA, and Elsevier, in October 2022. He delivered more than 150 invited talks, and chaired sessions in many national and international conferences. He acted as a reviewer in many reputed journals of IEEE, ACM, Elsevier, Springer, and Hindawi, and many reputed conferences. He has served as a guest editor in many international journals.



Studies (UPES), India, and the Dean (Faculty of IT and Science) of INTI International University, Malaysia. He has been with the IT industry for industry-academic collaboration, internships, placements, and workshops. He has executed the IBM Center of Education for Cloud Computing and Business Analytics, INTI International University, under Laureate International Universities, USA. He has presented and published many research papers in various conferences and journals. He has three Indian patents and three Australian patents to his credit. His research interests include business analytics, data mining, data warehouse, retail/e-commerce analytics, artificial intelligence, machine learning, and business process modeling. He has received the Mentor Award for the i-Talent Project Contest from the Confederation of Indian Industry (CII). He has played a vital role in organizing three international conferences, such as NGCT-2015 (UPES), ICQMOIT-2008 (ICFAI, India), and ICD-2019 (SUC, United Arab Emirates).

MANAS RANJAN PRADHAN (Member, IEEE) received the M.Tech. degree in computer science from Utkal University, India, and the Ph.D. degree in computer science from the University of Mysore, India. He has vast experience in teaching, research, and academic administration in India and abroad. He is currently with Skyline University College, Sharjah, United Arab Emirates. As an Academic Leader, he was the Head of the Program with the University of Petroleum and Energy



Engineering-Artificial Intelligence and Big Data Analytics, Marwadi University. He has a total of ten years of experience in both academia with some reputed universities, such as Ravenshaw University, and the software development field. He has published many research articles in internationally reputed journals and serves as a reviewer for many peer-reviewed journals. He has more than 50 patents on his credit. His research interests include multiprocessor scheduling along with different fields, such as data analytics, computer vision, machine learning, and the IoT. He is associated with various educational and research societies, such as IACSIT, CSI, IAENG, and ISC.

BISWARANJAN ACHARYA (Senior Member, IEEE) received the M.C.A. degree from IGNOU, New Delhi, India, in 2009, and the M.Tech. degree in computer science and engineering from the Biju Pattanaik University of Technology (BPUT), Rourkela, Odisha, India, in 2012. He is currently pursuing the Ph.D. degree in computer application with the Veer Surendra Sai University of Technology (VSSUT), Burla, Odisha. He is an Assistant Professor with the Department of Computer